Journal of Environmental Management 373 (2025) 123498

Contents lists available at ScienceDirect

Journal of Environmental Management

journal homepage: www.elsevier.com/locate/jenvman

Research article

Forensic determination of adhesive vinyl microplastics in urban soils

Glaucia I.A. Sebastião [a,b], Bárbara Rani-Borges [c], Jessica Dipold [d], Anderson Z. Freitas [d], Niklaus U. Wetter [d], Romulo A. Ando [c], Walter R. Waldman [e,*]

[a] Center of Human and Biological Sciences, Federal University of São Carlos, Sorocaba, Brazil
[b] Graduate Program in Planning and Use of Renewable Resources, Federal University of São Carlos, Sorocaba, Brazil
[c] Institute of Chemistry, Department of Fundamental Chemistry, University of São Paulo, São Paulo, Brazil
[d] Instituto de Pesquisas Energéticas e Nucleares, IPEN/CNEN, Av. Prof. Lineu Prestes, 2242, SP, Brazil
[e] Center of Science and Technology for the Sustainability, Federal University of São Carlos, Sorocaba, Brazil

ARTICLE INFO

Handling editor: Lixiao Zhang

Keywords:
Soil contamination
Microplastic hotspot
Weathering
Density separation

ABSTRACT

Plastic production and consumption hubs are mainly concentrated in urban centers, causing the soil in these places to become sinks of plastic fragments. Adhesive vinyl polymers are widely used in various commercial sectors and, to the best of our knowledge, this is the first study to investigate the potential for this type of material to form microplastics in urban soils. This proof-of-concept work started by studying the soil around a sign made of adhesive vinyl that had been exposed to the weather for eight years and showed evident signs of degradation, like cracking and color fading. We separated the microplastics with a two-step density separation protocol and selected only the microplastics targeted by this research, finding up to 5,570 fragments produced from 1 cm^2 of adhesive vinyl film. In the soil below the sign, we registered 5.6×10^4 fragments kg^{-1} of dry soil on its topsoil layer (0–10 cm), 1.2×10^4 fragments kg^{-1} in the 10–20 cm layer, and 1×10^4 fragments kg^{-1} in the 20–30 layer. At a distance of 1 and 2 m from the sign, the highest concentration of fragments was also in the topsoil, respectively 9.3×10^3 and 5.3×10^2 fragments kg^{-1}. We also observed that vertical and horizontal transport was not favored, causing the formation of hotspots near the source and that the area of the fragments did not influence vertical transport. Another important finding regarding the characterization technique is that degraded polyvinyl chloride is unlikely to be identified through FTIR without comparison to the source. Here, we presented a low-cost forensic assessment of the association between the presence of MPs and its source that can be used both for the development of public policies and for setting up quality controls for polluting companies. The results here presented reveal the need to rethink the use and types of materials used for visual identities and signage in urban environments.

1. Introduction

Microplastics (MPs) are emerging contaminants that have been increasingly gaining momentum in discussions surrounding anthropogenic impacts. They can enter several environments in their primary form, when they are intentionally produced smaller than 5 mm, or in their secondary form, when they are generated from the degradation of larger plastics. As more studies show the presence of microplastics (MPs) in places far from the hubs of plastics production and consumption, such as the Antarctic (Cincinelli et al., 2017), deep-sea sediments (Van Cauwenberghe et al., 2013), clouds (Wang et al., 2023), and caves (Hasenmueller et al., 2023; Balestra and Bellopede, 2022), more questions are raised regarding the impact of these emerging contaminants on ecosystems (UNEP, 2014). For instance, microplastics can pose a physical threat to the biota by obstructing gastrointestinal and respiratory tracts (Liza et al., 2024), a chemical threat through the release of additives (Luo et al., 2022) and transport of pollutants (Hu et al., 2022) and change the physical and chemical properties of ecosystems (Qiu et al., 2022).

Despite being found in remote regions, MPs are likely to be more abundant in populational hubs, which makes urban centers primarily responsible for the production and fate of MPs in the environment (Österlund et al., 2023). Indeed, urban soils act as pathways for MPs to flow into groundwater while acting as sinks for MPs (Qi et al., 2020; Guo et al., 2020). Therefore, studies involving the dispersion dynamics of plastic pollution in urban areas are essential for understanding how MPs are dispersed in different environmental compartments, supporting the

* Corresponding author.
E-mail address: walter@ufscar.br (W.R. Waldman).

https://doi.org/10.1016/j.jenvman.2024.123498
Received 8 July 2024; Received in revised form 20 November 2024; Accepted 25 November 2024
Available online 6 December 2024

Abbreviation

MP	microplastic
PVC	polyvinyl chloride

graffiti paint particles studied have a high density compared to other types of MPs, making them difficult to disperse and also to analyze using conventional density separation protocols, which demanded a customized separation method.

An example of a high-density polymer that fits in the previous description is polyvinyl chloride (PVC). In 2022, PVC accounted for 12.7% of global plastic production, which reached 400.3 million tons,

Fig. 1. Examples of everyday objects with visually degraded parts made of adhesive vinyl films: (A) No parking sign; (B) Parking banner; (C) Parking identification sign in a mall; (D) Traffic sign; (E) Sign made of adhesive vinyl that generated the MPs in the soil targeted in this study; (F) Magnification of E.

development of mitigation strategies (Koutnik et al., 2021).

Characteristics like shape, size, formulation, and density determine the potential of MPs to disperse. Additionally, the pathway through which they flow—such as air mass, groundwater movement, soil runoff, and water flow—also plays a role in the dispersal of fragments (Alfonso et al., 2021).

MPs with low transport capacity in soil are more likely not to be detected in monitoring studies far from urban sites and more prone to form hotspots as they remain concentrated close to the source of dispersion. An example of this phenomenon was studied by Xu et al. (2022), who reported the highest concentration in the literature of MPs in soil nearest the Mauerpark graffiti wall in Berlin (Xu et al., 2022). The

making it the third most produced type of plastic, only behind polypropylene (PP) (18.9%) and polyethylene [both low-density (PE-LD) and linear low density (PE-LLD)] (14.1%) (Plastics Europe, 2023). Nevertheless, despite being among the most produced types of plastic, PVC was detected in 25% of types of soil and sediment analyzed in a review (Koutnik et al., 2021). Since its high density (~1.5 g/cm^3) causes this material to deposit quickly into the sediment when released, it raises the alert to the potential for hotspot formation by PVC MPs. Furthermore, it is worth noting that PVC is a type of plastic that carries a high load of additives in its composition, making PVC MPs a relevant vector of pollutants (Ye et al., 2020).

One common application of PVC is in adhesive vinyl. These

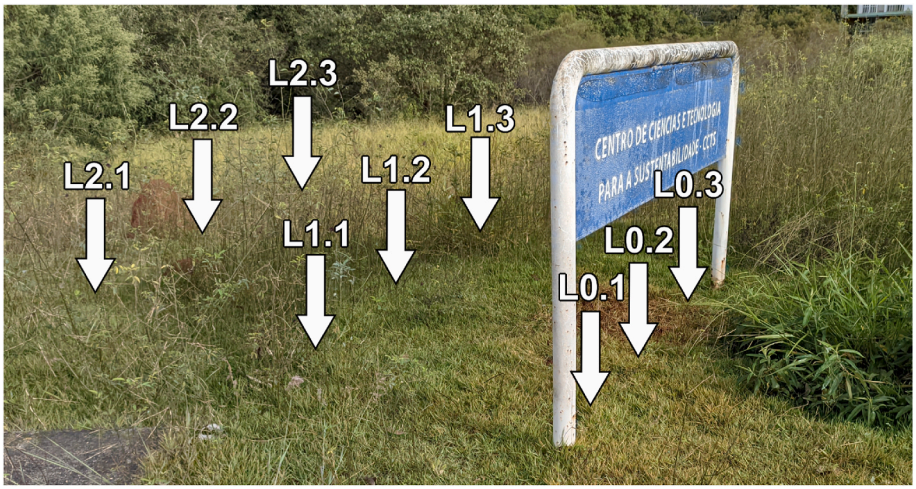

Fig. 2. Picture of the studied site, showing the location of the samples distant 0 m, 1 m, and 2 m from the MP source.

adhesives can be used for visual communication, car adhesives, and interior decoration (a few examples in Fig. 1). Despite being commonplace in urban centers, there is no record in the literature assessing the potential for MPs to form from these sources.

Studies investigating the fragmentation potential of plastic materials widely used in urban centers can aid in different ways in the context of the Sustainable Development Goals proposed by the United Nations, by contributing to the achievement of the following ones: SDG 11, "Sustainable cities and communities," by showcasing the need to replace these materials if harmful, SDG 12, "Responsible consumption and production," by indicating the pollution potential of sources widely used in urban contexts, and SDG 15, "Life on land," by providing evidence for the development of further studies aimed at enhancing the well-being of organisms and terrestrial systems."

Therefore, the aim of this study was to carry out an analysis on the soil exposed to a specific source—a sign coated with adhesive vinyl that was left outdoors for eight years—to see whether the fragmentation potential of this material could be contributing to plastic pollution on soil. Thus, the hypothesis of this study were: 1) the degradation of vinyl adhesive signs contributes to plastic pollution in the soil and 2) the protocol developed by Xu et al. (2022) (Xu et al., 2022) can be applied in forensic studies correlating the presence of microplastics and their origin.

2. Materials and methods

2.1. Collection of soil samples

Soil samples were collected in Sorocaba, São Paulo, Brazil (23°34′59.20″S, 47°31′31.94″W) around a sign containing an adhesive vinyl film that had been exposed to the weather for eight years. We noticed the whole blue area of the film was cracked, indicating that the polymer was highly degraded (Fig. 1E and F). To analyze horizontal transport, we collected samples from below the sign (0 m), 1 m, and 2 m distance from the back of the sign (Fig. 2). To analyze the vertical transport, we collected samples up to 30 cm deep, dividing the collection into three layers 10 cm deep (0–10 cm, 10–20 cm, and 20–30 cm). At each distance, the collection was carried out in triplicate with a soil sampler drill (Saci steel drill bit 1″ x 0–80 cm). Each site is identified in Fig. 2. Soil samples were dried in an oven at 50 °C for 48 h and then sieved through a 2 mm sieve. The sample code had the format LX.Y, with L standing for location, X standing for the distance from the sign in meters, and Y standing for the replicate number (Fig. 2).

2.2. Controls and precautions to avoid contamination

As long as MPs are everywhere, including inside laboratories (Noonan et al., 2023), we have adopted a number of precautions. All reverse osmosis water used throughout the experiments was filtered three times using membranes with pores of 5 μm in a vacuum filtration system, as well as we have done with the NaCl and NaBr saturated solutions. In addition, every step of processing the samples was performed inside a laminar flow hood whenever the soil needed to be exposed to air (except for weighings). This laminar flow hood was located in a room with controlled access of people where only cotton coats were allowed, and every time it needed to be used, a wet membrane was placed inside the laminar flow hood workspace to monitor the MPs deposited from the air as a control. Another precaution was to wash the falcon tubes, glassware, and tools three times with the filtered water mentioned earlier.

To avoid contamination of MPs by the salts (Kutralam-Muniasamy et al., 2023), we dissolved them in distilled water and then filtered these solutions three times through a 5 μm pore membrane. We evaporated this solution by heating it at a temperature below the boiling point in a laminar flow hood to obtain the MP-free salt and then collected the precipitate.

We also adopted controls for saline solutions used in density separation. These consisted of adding the same amount of solution to a previously cleaned Falcon tube. After going through the same procedures as the other tubes (shaking and centrifuging), we filtered these solutions and analyzed them under a stereomicroscope. This control was carried out three times, each corresponding to the distance of the collections (0 m, 1 m, and 2 m). All these procedural blanks can help to avoid MPs, while air deposition blanks are essential to track the quality of the working environment (Prata et al., 2021).

All controls adopted throughout the procedural and atmospheric deposition controls registered the absence of contamination by blue MPs. All the steps and precautions taken were necessary for this result, especially when cleaning the reagents and solvent. When manufactured, these products lack MP quality control and are packaged in plastic, increasing the risk of contamination (Liu et al., 2024).

While optimizing the experiment conditions, we noticed the unexpected presence of blue microplastics in the procedural controls, which could have come from the blue-capped Falcon tubes. To avoid this source of contamination, we replaced the original blue-capped Falcon tubes with orange-capped ones.

2.3. Separation and visualization of the microplastics

In order to separate the blue MPs from the soil, we adapted a customized two-step separation protocol developed by Xu et al. (2022) (Xu et al., 2022), which takes advantage of the density of a specific plastic to separate it from the other MPs and organic matter. Shortly, we collected plastic pieces from the source of MPs and determined the density that makes them float and sink, respectively 1.5 g/cm^3 (NaBr saturated solution) and 1.2 g/cm^3 (NaCl saturated solution). Then, we carried out the first step of separation, mixing 7.5 mL of NaCl saturated solution and 2.5 g of dry soil in a 15 mL Falcon tube, placed the tubes in an orbital shaker for 15 min at 67 rpm, and centrifuged them for 10 min at 1,600 rpm. After centrifugation, the supernatant containing the most organic matter and less dense MPs was discarded. The separation of the blue MPs was carried out using the Falcon tube containing soil wetted with the remaining NaCl solution, added with filtered water enough to reach the mark of 12 mL in the tube and enough NaBr to allow the observation of non-dissolved NaBr crystals after the 15 min of orbital shaking, which is the evidence of the saturation. Centrifugation for 10 min at 1,600 rpm was carried out and the supernatant separated. The whole protocol of the NaBr solution was repeated two more times to ensure the recovery of the blue MPs dragged along the soil during decantation. After the repetitions, the collected supernatants were transferred to a vacuum filtration system (membrane GVS, Nylon disk 47 mm 0.45 μm), and the membrane, after drying at room temperature, was examined in a Leica S8APO stereomicroscope for further analysis and measurements in the software ImageJ.

3. Microplastics identification

3.1. Polymer type in the microplastics

To identify the chemical composition of the polymer in the sign and the soil, we first removed fragments directly from the sign (Fig. 1E and F, and 2), and analyzed them by ATR-FTIR. We identified a coating on the polymer, potentially leading to misinterpretation, so we placed a paint fragment in a glass flask—previously cleaned with 90% acetone—immersed in ether in an ultrasound bath for 30 min. After the resin removal, it was possible to observe new bands and intensities, which were discussed later in the text. The same protocol with ether was applied to the particles found in the soil, and then we gathered the particles on the top of the reflective element for the measurement.

Measurements were recorded at room temperature using a FTIR spectrometer, model Alpha, in the region of 400–4000 cm^{-1}, with a DLATGS detector. The spectra were recorded with the ATR (attenuated

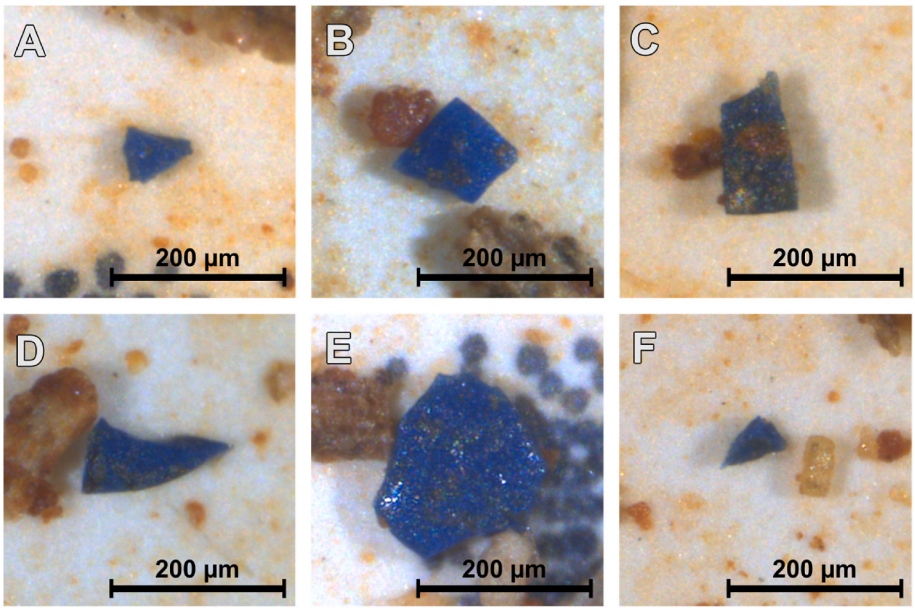

Fig. 3. Micrographs of blue fragments from the soil sampled below the adhesive vinyl film at the 0–10 cm depth, which are also examples of MPs with sharp edges (A–F). All the micrographs taken for this study are available in the Zenodo repository at the link: doi.org/10.5281/zenodo.10516559.

total reflection) module: ATR Platinum, equipped with a diamond crystal as a reflective element. The spectra were obtained through 64 accumulations with a resolution of 4 cm^{-1}.

3.2. Pigment determination

Raman spectra were measured using the labRAM HR Evolution (HORIBA) with lasers of different wavelengths (473 nm, 532 nm, 633 nm, and 785 nm) and a 50× long-range objective (NA = 0.55). The resistance of each material was tested for different power levels of each laser to obtain the best signal for the spectra without damaging the material. We used a starting position on the spectrometer to allow the peaks in the polymer identification region (fingerprint) to be observed around 1600 cm^{-1}. For the final spectrum measurement, we used the region from 200 cm^{-1} to 3200 cm^{-1}, allowing the observation of the entire common polymer fingerprint region and the C-H stretching region.

The parameters were optimized to obtain the spectra of the samples, mainly by checking the appropriate laser wavelength and the maximum power that the sample could bear without damage. The chosen wavelength was 633 nm, with 10 mW power, 5 s integration time and 10 accumulations, generating spectra with high signal-to-noise ratio and making identification possible. A filter was used, which automatically identified and removed any spikes due to cosmic rays by comparing the spectra from the different accumulations.

A baseline and a noise filter were applied using the tools in the micro-Raman software itself (Labspec) or a Matlab® code. The compounds in the spectra were identified using the Knowitall® database.

3.3. Data visualization

The graphs were made with OriginPro 2024 and designed using a color-blindness accessibility guide (Pereira, 2021), to represent color and patterns to provide readable material for color-blind people.

3.4. Statistical analysis

We performed a Kruskal-Wallis test ($p < 0.05$) in GraphPad Prism 8.0 software for all MPs sizes comparisons, as the data did not satisfy the assumptions required for a parametric test (normality and homoscedasticity).

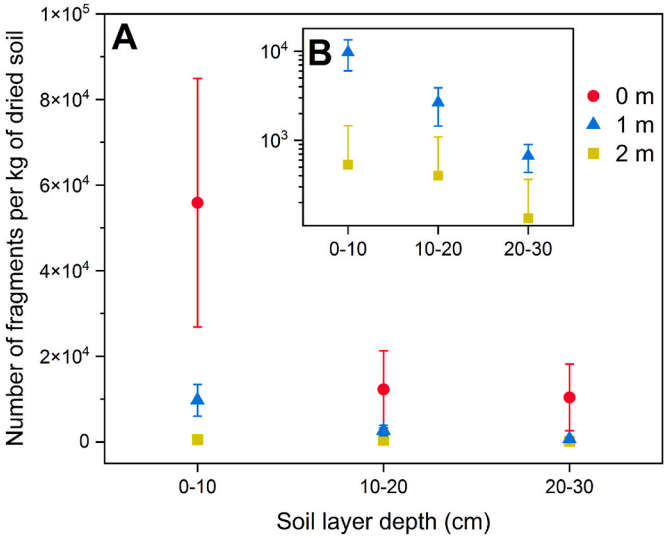

Fig. 4. A) Number of fragments in 1 kg of dry soil (triplicates combined for averaging) at each soil layer depth. The topsoil layer was the most contaminated by blue MPs, with the soil below the sign (0 m) showing the highest number of MPs, demonstrating the ability of the fragments from adhesive vinyl films to form hotspots near the source. B) Magnification of graph A to better visualize the data at 1 and 2 m. The data is available in Supplementary Material, file all_data.pdf, tab "Number of Fragments".

4. Results and discussion

4.1. Microplastics quantification

Adhesive vinyls are widely used for visual identification and, therefore, widely manufactured and applied everywhere, even in outdoor spaces, where they degrade and break (Fig. 1). With this in mind, we decided to investigate the forensic tracking of this sort of MPs coming from a specific source. Setting a causal nexus between the source and the presence in the environment is essential in the framework of the current

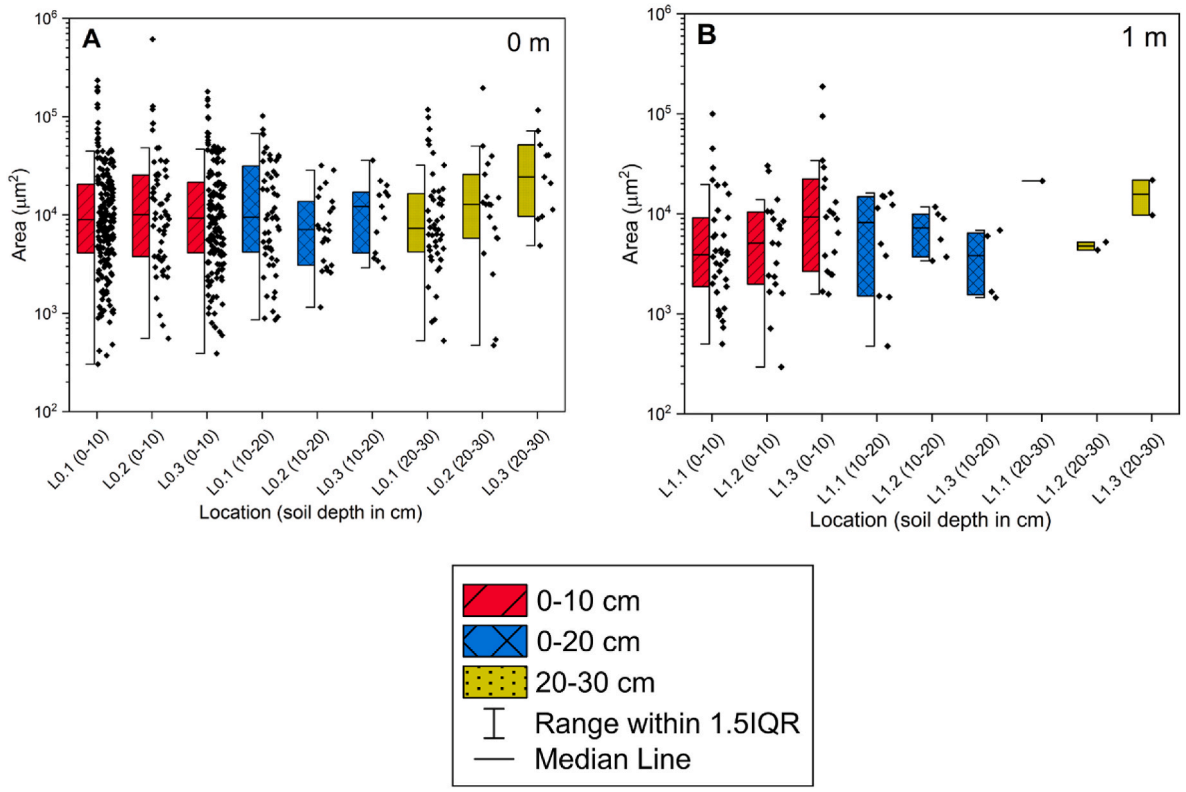

Fig. 5. Dispersion of areas as a function of depth for all triplicates at a distance of 0 m (A) and 1 m (B) from the sign. No significant differences were found between the triplicates within each distance by applying the Kruskal-Wallis test. The complete figure containing the information for 2 m is available in Supplementary Material, file auxiliary_figures.pdf, Fig. S1.

discussions about plastic pollution, mainly to determine the problematic products because of the potential release of MPs (UNEP, 2023). Also, developing protocols to set a causal nexus between the MPs in the environment and the source from where they came from is a tool for future accountability in cases of environmental pollution investigation.

The initial protocol used the plastic source to customize the separation of the MPs of interest using density. We determined that the pieces of plastic from the source sank in the NaCl saturated solution (1.2 g/cm^3) and floated in the NaBr saturated solution (1.5 g/cm^3). Using the NaCl-saturated solution as a first step leads to removing the less dense MPs, like PP and LDPE, and most organic matter, cleaning the potential contamination of the MPs of interest with other MPs and organic matter in excess. In this particular study, this step also removed enough organic matter to avoid the digestion step, making the protocol simpler, faster, and less expensive. Additionally, the reagents used in the digestion step might affect the shape of polymers and their chemical composition (Pfeiffer and Fischer, 2020; Dehaut et al., 2016). Representative pictures of the visualization conditions of MPs found in this study are in Fig. 3A–F. Only the blue fragments, the color of the plastic in the source, were quantified.

The mean number of fragments at each depth and distance from the sign can be seen in Fig. 4. At the distance of 0 m, we registered 5.6×10^4 fragments kg^{-1} of dry soil on its topsoil layer (0–10 cm), 1.2×10^4 fragments kg^{-1} of dry soil in the 10–20 cm layer, and 1×10^4 fragments kg^{-1} of dry soil in the 20–30 layer. At a distance of 1 and 2 m from the sign, the highest concentration of fragments was also in the topsoil, respectively 9.3×10^3 and 5.3×10^2 fragments kg^{-1}. To check this magnitude in contrast to the literature, we compared the highest concentration of fragments found in this study—an average of 5.6×10^4 kg^{-1} of dry soil at 0 m in 0–10 cm depth—with the MPs concentrations in soil samples of urban soil and street dust as analyzed by the review of Koutnik et al. (2021) (Koutnik et al., 2021). We found that the concentration encountered here is above the upper quartile of the gathered

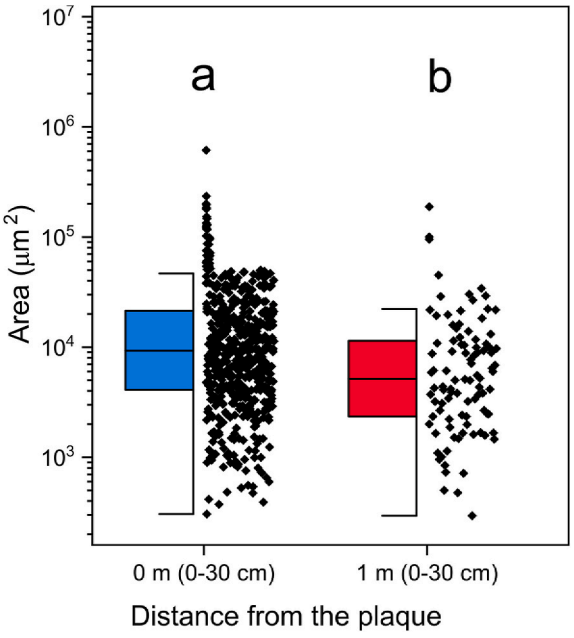

Fig. 6. Area (µm^2) of blue fragments at each distance from the sign. The farther the source, the smaller the fragments. Different letters indicate significant differences between the area in fragments at 0 m and 1 m. Due to the small number of values, no comparisons were made for fragments at 2 m. The complete figure containing the information for 2 m is available in Supplementary Material, file auxiliary_figures.pdf, Fig. S2.

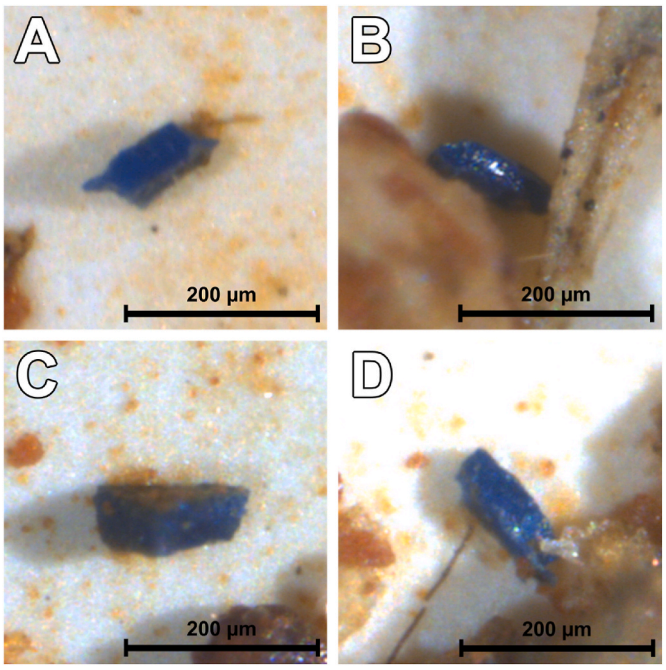

Fig. 7. Examples of MPs inclined on the membrane that allowed its thickness to be measured. The complete set of pictures that were used for measuring thickness is available in Supplementary Material, file auxiliary_figures.pdf, Fig. S3, as well as the measurements, available in file all_data.pdf, tab "Thickness".

literature. This concentration is even more significant if we consider that we are only quantifying one type of microplastic, discarding the most found microplastics in literature and also the most produced, like polypropylene and polyethylene (Koutnik et al., 2021; Plastics Europe, 2023; Maharana et al., 2020; Liu et al., 2018), in the first step of separation using the NaCl-saturated solution.

The farther from the source, the fewer fragments are on the soil, which indicates that horizontal transport is not the leading cause of distribution. Density is one of the fundamental properties that determine MP transport (Koutnik et al., 2021), and the higher density of blue MPs makes them likely to settle vertically. Fragments far from the sign probably got there through the wind, surface water runoff in the soil, or even through bioturbation (Nie et al., 2022; Huerta Lwanga et al., 2017; Han et al., 2022).

To check if the MP size could play a role in the transport, we measured the area of every fragment observed on the membrane and compared them to check if the size varied according to the depth for all locations (Fig. 5). We first compared the same depths at each distance (triplicates). As no significant differences were found (Fig. 5A and B), we expanded the analysis by comparing the complete set of triplicates (9 samples) for each distance. This also revealed no significant differences as a function of the depth at 0 m (Fig. 5A) and at 1 m (Fig. 5B), meaning that the size does not influence the vertical transport. This result contradicts what we would expect if we consider that the smaller MPs are reported as having stronger vertical transport (Liu et al., 2024). The results at 2 m were not considered for comparison and were not included in Figs. 5 and 6 since the sample size was small.

Since there was no significant difference in the area of the particles at a given distance, we combined the area of all the fragments from the three triplicates within each distance and compared the areas between the distances, but only the most significant results are shown in Fig. 6 (complete figure is available in Supplementary Material, file auxiliary_figures.pdf, Fig. S2). We found that there was a difference between the area of the fragments obtained at 0 m and 1 m, indicating the area decreases as a function of the distance from the source of contamination,

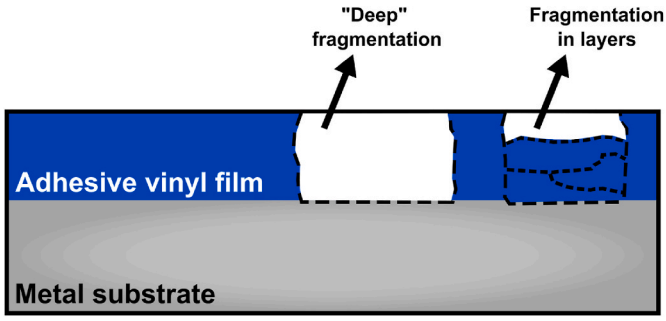

Fig. 8. Scheme representing our hypothesis for two different fragmentation dynamics for forming MPs from adhesive vinyl films from a transverse plane. Here, we consider deep fragmentation as the complete breaking of the fragment from the surface to the substrate and fragmentation in layers as the partial breaking of the fragment's extension. The white areas represent parts of the film that have detached.

which may indicate that smaller particles have a greater dispersion capacity than the larger ones.

4.2. Potential of fragmentation

Since the framework under study here is the collection of MPs originated from a given source, we attempted to estimate the area of the source needed to produce the MPs quantified so far. Firstly, we chose the location with the highest concentration of MP, 0 m distance, and summed the area of all fragments found there. Then, we extrapolated the sum of the fragments found in 7.5 g (2.5 for each layer) to 1 kg (raw data available in Supplementary Material, file all_data.pdf, tab "Soil microplastics") to allow comparison with the literature. Finally, the value obtained in μm^2 is converted to cm^2 to make it relatable. The final result is the 26,178 fragments generated from 4.7 cm^2 (or 5,570 fragments from 1 cm^2) of the plastic sign.

Adding to the above-mentioned approach, we found evidence in the MPs inclined or verticalized on the membrane (Fig. 7, taken from a more extensive set of pictures available in Supplementary Material, file auxiliary_figures.pdf, Fig. S3) that the thickness varies from 20 to 40 µm, averaging 30 ± 7 µm. To check if the thickness is the same as in the sign, we measured the thickness of the most preserved film piece in the sign–a place shadowed by the metallic structure and still flexible, as opposed to the rest of the sign–and the average thickness was 60 ± 17 µm (pictures and measurements in Supplementary Material, file auxiliary_figures.pdf, Fig. S4). It shows that fragmentation can happen not only through the breakage of the film to the extension of the thickness but also through erosion of layers smaller than the thickness, as represented in Fig. 8.

Because of the difference between the thickness of the film in the sign and the MPs collected from the soil, the estimation of 4.7 cm^2 producing 26,178 microplastics is an overestimation. One central point to note is that we do not know the extent to which each of the processes illustrated in Fig. 8 occurs, still, the scenario is even more worrying since the area estimated earlier in the text generates a larger number of MPs.

4.3. Microplastics identification

Strategically, to establish a nexus between the MPs collected from the soil and their source, we carried out analysis using two types of vibrational spectroscopies: infrared for the polymer type characterization and degradation assessment and Raman for the analysis of the strong fluorescence of the blue pigment as a probe for matching the MP and its source by the presence of the same additive.

The FTIR analysis of the MP collected from the soil and the source in the sign led to the spectra in Fig. 9A and C, respectively. We cannot find a fit for the polymer identity there, mainly because there was no signal in the region between 2800 and 3100, attributed to the C-C and C-H bonds.

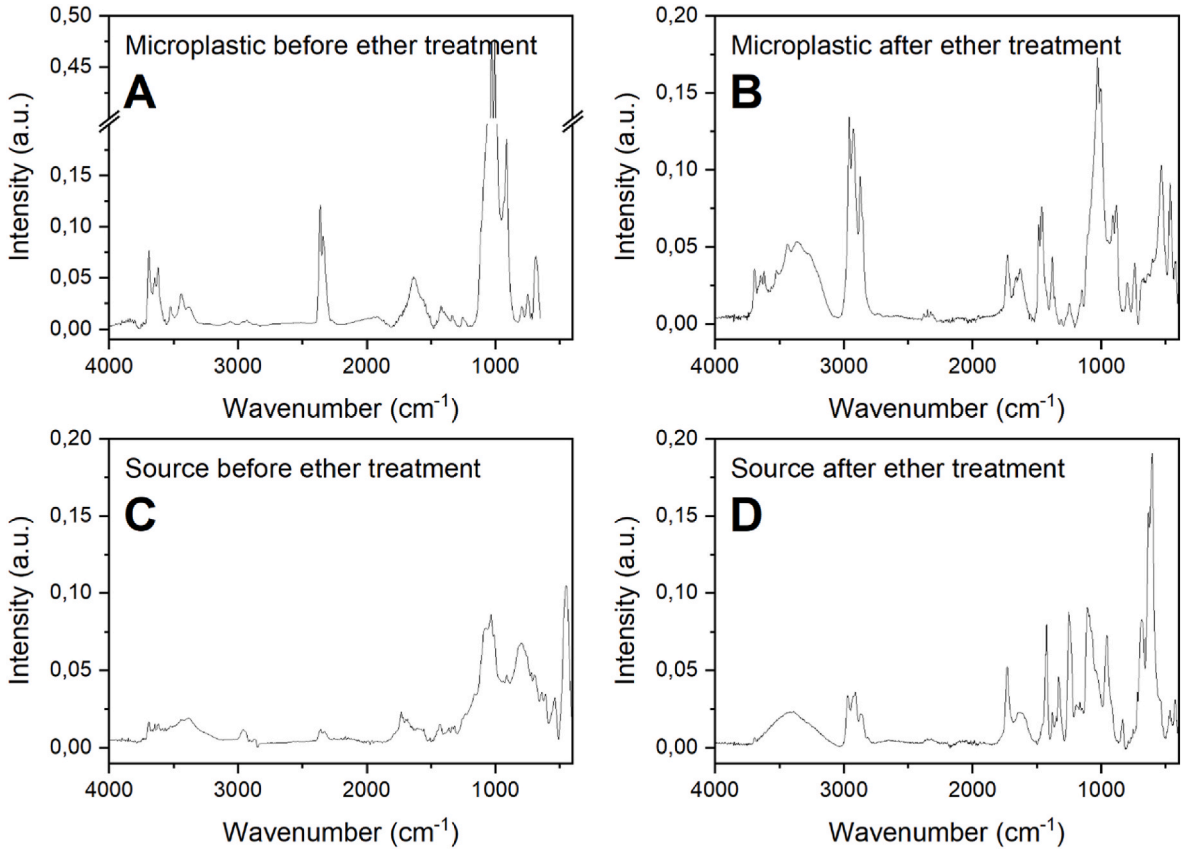

Fig. 9. FTIR spectra of A) the MP collected from the soil; B) the same sample in A after treatment with ether to remove interferents; C) the plastic collected directly from the source; D) the same sample in C after treatment with ether to remove interferents. A is out of scale compared to the spectra B, C, and D to allow visualization of the peak absorption.

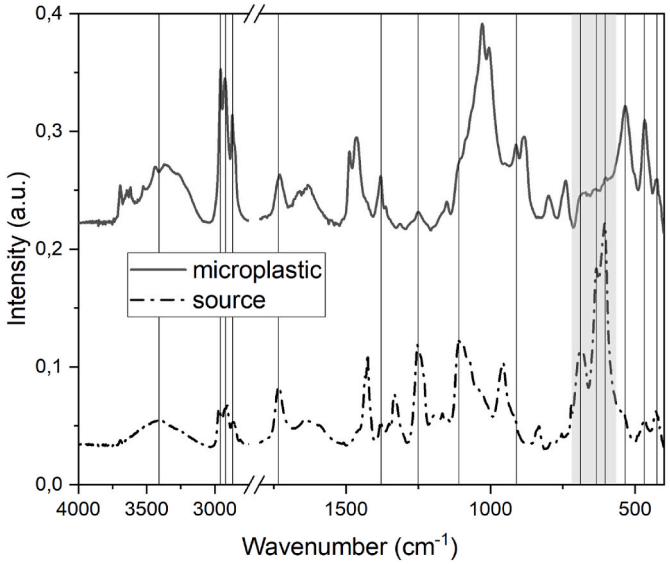

Fig. 10. FTIR spectra of the MPs collected in the soil (solid line) and a piece of the sign (dashed line). The spectra were displaced in the y-axis for a better visualization. All the lines crossing the graph show the bands occurring in both spectra. The gray highlight shows the bands attributed to the bond C-Cl.

Since it is usual to have adhesives under or resins over the film, we processed the samples using ether to remove any potential interferents. Then, we could observe the bands that determined the polymer type in the MPs (Fig. 9B) and the sign (Fig. 9D).

By comparison with the work of Abu-Saied et al. (2019) (Abu-Saied et al., 2019), we identified the polymeric composition of the MP and its source as being made of Poly (vinyl chloride) and Polyacrylic Acid. Fig. 10 shows the spectra of MP and its source, and all the bands coinciding in both, including shoulders, are identified by a line, showing the similarity of composition between both.

The main bands of the Polyacrylic Acid (Abu-Saied et al., 2019) are the ones at 1428 and 960 cm^{-1}, attributed respectively to the OH in-plane and out-of-plane deformations; at 1725 cm^{-1} attributed to the carbonyl band; and the range between 3030 and 3700 cm^{-1} attributed to the hydroxyl stretching. Regarding the PVC, the main bands for its identification are the ones at 1252 and 1328 cm^{-1}, attributed to the Hydrogen bonded to the group C-Cl, whereas the bands at 607, 639, and 682 cm^{-1} are the ones attributed to the bonding C-Cl (Beltrán and Marcilla, 1997).

The bands related to the C-Cl from PVC are particularly interesting when comparing the source and the microplastic. The former has the bands still clearly seen in the spectra of the source, the most preserved against degradation, and the latter has these same bands decreased to the point of prevention of the polymer identification. This happens because of the mechanism of dehydrochlorination, which occurs during PVC degradation, with the removal of HCl and the formation of a vinyl group (Beltrán and Marcilla, 1997). This result is particularly relevant because investigating the MPs close to the source allowed us to identify the polymer that originated the microplastics. Because of the identification of the polymer in the source, the least intense bands that could be mistaken as noise or contamination can make sense chemically as evidence of the residual C-Cl groups and the degradation level of the MPs. Notably, without knowing the source, the polymer would not have been identified only with the MP spectra.

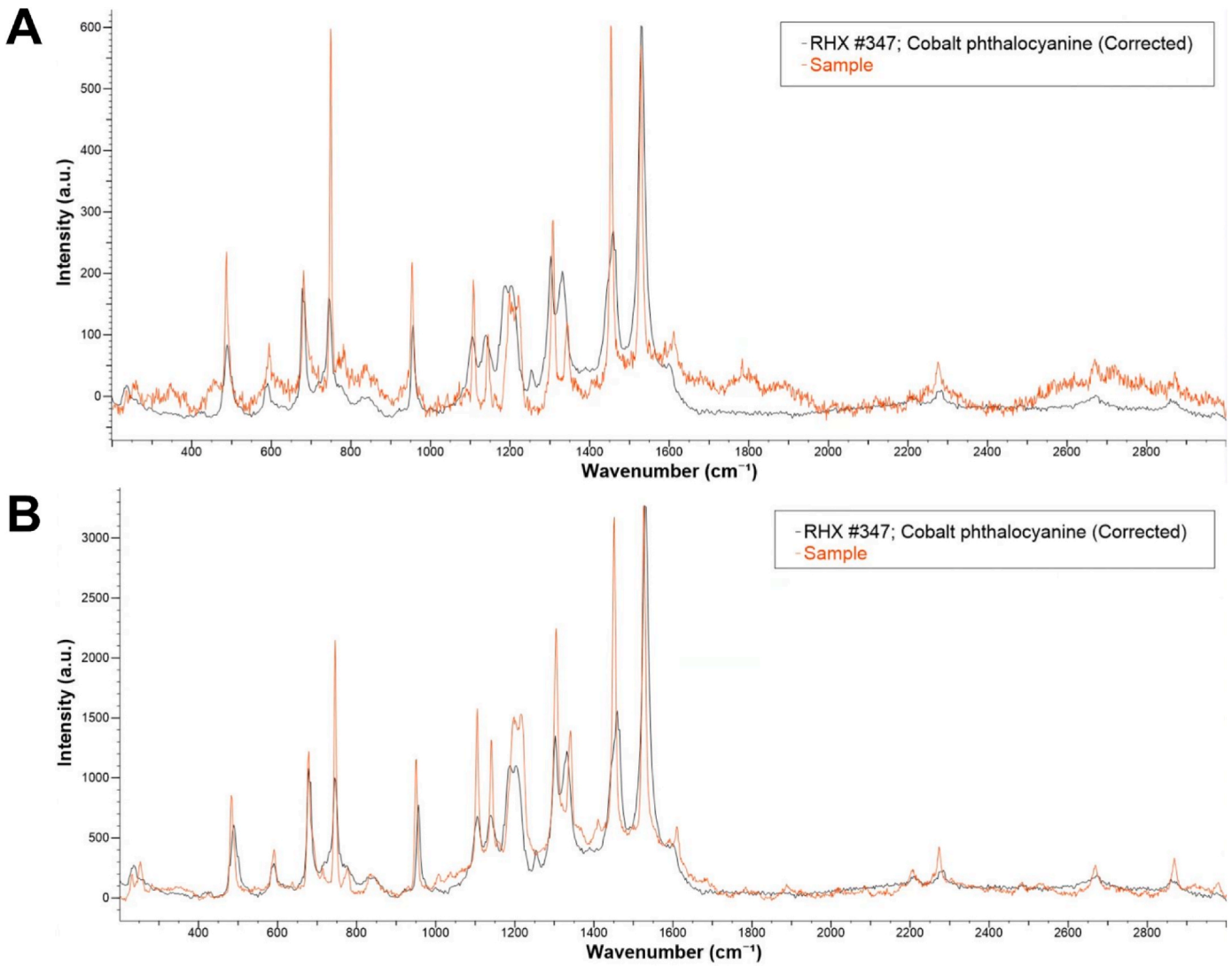

Fig. 11. Raman spectra for A) the MP collected from the soil, and B) the piece of the film on the sign.

Because of the strong Raman signal emitted from the pigment, the identification of the polymer itself by Raman spectroscopy was not possible, although this phenomenon allowed a more interesting feature for the forensic approach: the identification of the pigment itself. The Raman analysis yielded the spectra of the MP (Fig. 11A) and the plastic piece from the sign (Fig. 11B), matching the same additive, the blue pigment cobalt phthalocyanine. This information, added to the FTIR spectra, led to the forensic match needed to confirm the nexus between the MPs and the source.

5. Conclusion

In the studied conditions, a single PVC sign contributed to 5.6×10^4 fragments.kg^{-1} of dry soil in the topsoil layer. Given the forensic association, we could correlate for the first time the quantification of the fragments from a specific source: 5.57×10^3 from 1 cm^2 of the source. Also, we could forensic prove, using vibrational spectroscopies, the forensic linkage between the contamination and the source. Regarding transport, for the specific context studied here, fragments size did not influence horizontal or vertical displacement. The development of a forensic approach from the tools already available can provide a tool for polluters accountability, parameters for environmental quality control in products for outdoor purposes and the lifespan determination for outdoor contexts.

CRediT authorship contribution statement

Glaucia I.A. Sebastião: Writing – review & editing, Writing – original draft, Visualization, Validation, Methodology, Investigation, Formal analysis, Conceptualization. **Bárbara Rani-Borges:** Writing – review & editing, Investigation. **Jessica Dipold:** Writing – review & editing, Investigation. **Anderson Z. Freitas:** Writing – review & editing, Investigation. **Niklaus U. Wetter:** Writing – review & editing, Investigation. **Romulo A. Ando:** Writing – review & editing, Investigation. **Walter R. Waldman:** Writing – review & editing, Writing – original draft, Supervision, Funding acquisition, Formal analysis, Conceptualization.

Supplementary material

File all_data.pdf: tab “Soil microplastics” contains the sizes of all microplastics measured; tab “Number of fragments” contains the quantification of fragments number for all the collection sites; tab “Thickness” contains all the thickness measured with the association to the pictures.

File auxiliary_figures.pdf: contains a figure for the dispersion of areas as a function of depth for all triplicates (S1); a figure for the area of blue fragments at each distance from the sign (S2); a figure for micrographs of particles that were facing upwards in the membrane (S3); and a figure

for thickness of three portions of a preserved film piece in the sign.

All the pictures used for all the size measurements are available in the Zenodo repository at the link: https://doi.org/10.5281/zenodo.10516559.

Funding sources

This work was supported by: Project MARTMA-FINEP (0152/21) WRW; FAPESP Thematic Project (2022/12104-4; 2022/11983-4) WRW and RAA; FAPESP Fellowship (2022/15586-0; 2017/50332-0) BRB and NUW; FAPESP-EMU (2018/19240-5) AZF; CNPq Grant (406391/2021-1) WRW; CNPq Grant (314079/2021-1) AZF; CNPq and FAPESP for the INCT Circularidade (406925/2022-4) WRW; IPEN grant (2020.06. IPEN.33.PD) NUW; CAPES (Finance Code 001) for the fellowship GIAS.

Declaration of competing interest

The authors declare that they have no known competing financial interests or personal relationships that could have appeared to influence the work reported in this paper.

Acknowledgments

ProPQ (UFSCar); Prof. Dr. Eliane Arruda for the usage of the stereomicroscope and suggestions; Prof. Dr. Andréa Onofre for the suggestions; Prof. Dr. Francisco Strixino for the usage of the centrifuge; MSc Mussa Issufo for the support in taking soil samples; for both the dean of the Sorocaba campus and the Center of the Sciences and Technology for Sustainability for delaying the replacement of the cracked sign so we could finish the research project.

Appendix A. Supplementary data

Supplementary data to this article can be found online at https://doi.org/10.1016/j.jenvman.2024.123498.

Data availability

All the data collected in this work is available for consultation.

References

Abu-Saied, M., Fahmy, A., Morgan, N., Qutop, W., Abdelbary, H., Friedrich, J.F., 2019. Enhancement of poly(vinyl chloride) electrolyte membrane by its exposure to an atmospheric dielectric barrier discharge followed by grafting with polyacrylic Acid. Plasma Chem. Plasma Process. 39 (6), 1499–1517. https://doi.org/10.1007/s11090-019-10017-6.

Alfonso, M.B., Arias, A.H., Ronda, A.C., Piccolo, M.C., 2021. Continental microplastics: presence, features, and environmental transport pathways. Sci. Total Environ. 799, 149447. https://doi.org/10.1016/j.scitotenv.2021.149447.

Balestra, V., Bellopede, R., 2022. Microplastic pollution in show cave sediments: first evidence and detection technique. Environ. Pollut. 292, 118261. https://doi.org/10.1016/j.envpol.2021.118261.

Beltrán, M., Marcilla, A., 1997. Fourier transform infrared spectroscopy applied to the study of PVC decomposition. Eur. Polym. J. 33 (7), 1135–1142. https://doi.org/10.1016/S0014-3057(97)00001-3.

Cincinelli, A., Scopetani, C., Chelazzi, D., Lombardini, E., Martellini, T., Katsoyiannis, A., Fossi, M.C., Corsolini, S., 2017. Microplastic in the surface waters of the Ross Sea (Antarctica): occurrence, distribution and characterization by FTIR. Chemosphere 175, 391–400. https://doi.org/10.1016/j.chemosphere.2017.02.024.

Dehaut, A., Cassone, A.-L., Frère, L., Hermabessiere, L., Himber, C., Rinnert, E., Rivière, G., Lambert, C., Soudant, P., Huvet, A., Duflos, G., Paul-Pont, I., 2016. Microplastics in seafood: benchmark protocol for their extraction and characterization. Environ. Pollut. 215, 223–233. https://doi.org/10.1016/j.envpol.2016.05.018.

Guo, J.-J., Huang, X.-P., Xiang, L., Wang, Y.-Z., Li, Y.-W., Li, H., Cai, Q.-Y., Mo, C.-H., Wong, M.-H. Source, 2020. Migration and toxicology of microplastics in soil. Environ. Int. 137, 105263. https://doi.org/10.1016/j.envint.2019.105263.

Han, N., Zhao, Q., Ao, H., Hu, H., Wu, C., 2022. Horizontal transport of macro- and microplastics on soil surface by rainfall induced surface runoff as affected by vegetations. Sci. Total Environ. 831, 154989. https://doi.org/10.1016/j.scitotenv.2022.154989.

Hasenmueller, E.A., Baraza, T., Hernandez, N.F., Finegan, C.R., 2023. Cave sediment sequesters anthropogenic microparticles (including microplastics and modified cellulose) in subsurface environments. Sci. Total Environ. 893, 164690. https://doi.org/10.1016/j.scitotenv.2023.164690.

Hu, L., Zhao, Y., Xu, H., 2022. Trojan horse in the intestine: a review on the biotoxicity of microplastics combined environmental contaminants. J. Hazard Mater. 439, 129652. https://doi.org/10.1016/j.jhazmat.2022.129652.

Huerta Lwanga, E., Gertsen, H., Gooren, H., Peters, P., Salánki, T., Van Der Ploeg, M., Besseling, E., Koelmans, A.A., Geissen, V., 2017. Incorporation of microplastics from litter into burrows of Lumbricus terrestris. Environ. Pollut. 220, 523–531. https://doi.org/10.1016/j.envpol.2016.09.096.

Koutnik, V.S., Leonard, J., Alkidim, S., DePrima, F.J., Ravi, S., Hoek, E.M.V., Mohanty, S. K., 2021. Distribution of microplastics in soil and freshwater environments: global analysis and framework for transport modeling. Environ. Pollut. 274, 116552. https://doi.org/10.1016/j.envpol.2021.116552.

Kutralam-Muniasamy, G., Shruti, V.C., Pérez-Guevara, F., Roy, P.D., Elizalde-Martínez, I., 2023. Common laboratory reagents: are they a double-edged sword in microplastics research? Sci. Total Environ. 875, 162610. https://doi.org/10.1016/j.scitotenv.2023.162610.

Liu, M., Lu, S., Song, Y., Lei, L., Hu, J., Lv, W., Zhou, W., Cao, C., Shi, H., Yang, X., He, D., 2018. Microplastic and mesoplastic pollution in farmland soils in suburbs of Shanghai, China. Environ. Pollut. 242, 855–862. https://doi.org/10.1016/j.envpol.2018.07.051.

Liu, Y., Han, J., Wang, Y., Li, A., Zhao, J., Su, Y., Shen, L., Xing, B., 2024. Suspected sources of microplastics and nanoplastics: contamination from experimental reagents and solvents. Water Res. 249, 120925. https://doi.org/10.1016/j.watres.2023.120925.

Liza, A.A., Ashrafy, A., Islam, Md.N., Billah, Md.M., Arafat, S.T., Rahman, Md.M., Karim, Md.R., Hasan, Md.M., Promie, A.R., Rahman, S.M., 2024. Microplastic pollution: a review of techniques to identify microplastics and their threats to the aquatic ecosystem. Environ. Monit. Assess. 196 (3), 285. https://doi.org/10.1007/s10661-024-12441-4.

Luo, H., Liu, C., He, D., Sun, J., Li, J., Pan, X., 2022. Effects of aging on environmental behavior of plastic additives: migration, leaching, and ecotoxicity. Sci. Total Environ. 849, 157951. https://doi.org/10.1016/j.scitotenv.2022.157951.

Maharana, D., Saha, M., Dar, J.Y., Rathore, C., Sreepada, R.A., Xu, X.-R., Koongolla, J.B., Li, H.-X., 2020. Assessment of micro and macroplastics along the west coast of India: abundance, distribution, polymer type and toxicity. Chemosphere 246, 125708. https://doi.org/10.1016/j.chemosphere.2019.125708.

Nie, C., Yang, J., Sang, C., Xia, Y., Huang, K., 2022. Reduction performance of microplastics and their behavior in a vermi-wetland during the recycling of excess sludge: a quantitative assessment for fluorescent polymethyl methacrylate. Sci. Total Environ. 832, 155005. https://doi.org/10.1016/j.scitotenv.2022.155005.

Noonan, M.J., Grechi, N., Mills, C.L., De, A.M.M., Ferraz, M., 2023. Microplastics analytics: why we should not underestimate the importance of blank controls. Microplast. Nanoplast. 3 (1), 17. https://doi.org/10.1186/s43591-023-00065-3.

Österlund, H., Blecken, G., Lange, K., Marsalek, J., Gopinath, K., Viklander, M., 2023. Microplastics in urban catchments: review of sources, pathways, and entry into stormwater. Sci. Total Environ. 858, 159781. https://doi.org/10.1016/j.scitotenv.2022.159781.

Pereira, Thiovane, 2021. Guia de Acessibilidade Cromática Para Daltonismo: Princípios Para Profissionais Da Indústria Criativa. Santa Maria.

Pfeiffer, F., Fischer, E.K., 2020. Various digestion protocols within microplastic sample processing—evaluating the resistance of different synthetic polymers and the efficiency of biogenic organic matter destruction. Front. Environ. Sci. 8, 572424. https://doi.org/10.3389/fenvs.2020.572424.

Plastics Europe, 2023. Plastics – the fast facts 2023. https://plasticseurope.org/knowledge-hub/plastics-the-fast-facts-2023/.

Prata, J.C., Reis, V., Da Costa, J.P., Mouneyrac, C., Duarte, A.C., Rocha-Santos, T., 2021. Contamination issues as a challenge in quality control and quality assurance in microplastics analytics. J. Hazard Mater. 403, 123660. https://doi.org/10.1016/j.jhazmat.2020.123660.

Qi, R., Jones, D.L., Li, Z., Liu, Q., Yan, C., 2020. Behavior of microplastics and plastic film residues in the soil environment: a critical review. Sci. Total Environ. 703, 134722. https://doi.org/10.1016/j.scitotenv.2019.134722.

Qiu, Y., Zhou, S., Zhang, C., Zhou, Y., Qin, W., 2022. Soil microplastic characteristics and the effects on soil properties and biota: a systematic review and meta-analysis. Environ. Pollut. 313, 120183. https://doi.org/10.1016/j.envpol.2022.120183.

UNEP, 2014. Emerging Issues in Our Global Environment; Nairobi.

UNEP, 2023. Zero Draft Text of the International Legally Binding Instrument on Plastic Pollution, Including in the Marine Environment. UNEP/PP/INC.3/4, United Nations Environment Programme: Nairobi, pp. 8–10. https://wedocs.unep.org/bitstream/handle/20.500.11822/43239/ZERODRAFT.pdf.

Van Cauwenberghe, L., Vanreusel, A., Mees, J., Janssen, C.R., 2013. Microplastic pollution in deep-sea sediments. Environ. Pollut. 182, 495–499. https://doi.org/10.1016/j.envpol.2013.08.013.

Wang, Y., Okochi, H., Tani, Y., Hayami, H., Minami, Y., Katsumi, N., Takeuchi, M., Sorimachi, A., Fujii, Y., Kajino, M., Adachi, K., Ishihara, Y., Iwamoto, Y., Niida, Y., 2023. Airborne hydrophilic microplastics in cloud water at high altitudes and their role in cloud formation. Environ. Chem. Lett. 21 (6), 3055–3062. https://doi.org/10.1007/s10311-023-01626-x.

Xu, Y., Rillig, M.C., Waldman, W.R., 2022. New separation protocol reveals spray painting as a neglected source of microplastics in soils. Environ. Chem. Lett. 20 (6), 3363–3369. https://doi.org/10.1007/s10311-022-01500-2.

Ye, X., Wang, P., Wu, Y., Zhou, Y., Sheng, Y., Lao, K., 2020. Microplastic acts as a vector for contaminants: the release behavior of dibutyl phthalate from polyvinyl chloride

pipe fragments in water phase. Environ. Sci. Pollut. Res. 27 (33), 42082–42091. https://doi.org/10.1007/s11356-020-10136-0.